



**K. N. Toosi University of Technology**  
**Faculty of Electrical Engineering**

## **Modeling the Hemodynamic Response – A Tutorial**

By: Benyamin Harkinezhad

Fall 2018

[The material in this tutorial is based on standard curriculum of K. N. Toosi University of Technology, Faculty of Electrical Engineering. For more information, please write to Benyamin Harkinezhad: [harki\\_ben@email.kntu.ac.ir](mailto:harki_ben@email.kntu.ac.ir)]

# Modeling the Hemodynamic Response

---

## Outline

1. Introduction
2. Definition
3. Model
4. Summary
5. References

## Introduction

The human body is an example of a powerful control system. Every task that is performed in the body, no matter how trivial it seems, involves complex and accurate control mechanisms. Although we perform this control unconsciously, it is worthwhile to be familiarized with the processes involved even if merely for the appreciation of the complexities our bodies. Nevertheless, an insight into the control mechanisms involved in the motion of body parts, provides us with valuable information on the working of the human brain.

Physical activity requires a great deal of control. As an example, in the case of a simple motion such as moving an arm to a certain position, position control as well as velocity control of the separate links of which the arm is comprised, is required. This in turn involves the control of muscle length and the way it changes. Additionally, contracting the muscle requires energy, which has to be accounted for by the brain. The latter issue is what we will consider in what follows.

In order to keep functioning efficiently, the tissues involved in the activity have to be provided with excess nutrients such as oxygen and glucose, which they will combine to produce energy. Thus, the blood flow to these tissues has to be increased in order to retain a condition of homeostasis. Homeostasis refers to a system's ability to regulate its internal environment and

maintain a constant condition of properties like temperature and pH. This change in the blood flow to a certain tissue due to neural activation is called the hemodynamic response.

In this tutorial, we will discuss the hemodynamic response and how it is modeled. First we will explain what the hemodynamic response is and what does the typical hemodynamic response function look like. Next we will go on to give a simple description on how the hemodynamic response is measured. Having clarified the meaning of the hemodynamic response, we will present mathematical models proposed to describe this effect. Finally, a summary of the disclosed information is given.

## **Definition**

As stated in the introduction, hemodynamic response refers to the adjustment of blood flow to tissues in stress in order to supply them with the necessary nutrients to perform an action. When the neuron attached to a certain tissue, say a muscle, is stimulated, blood flow to this tissue increases, resulting in a rise in the so-called hemodynamic response function (HRF). What this function actually represents will be explained soon. As the needs for the neuronal activity are met, blood flow returns to its baseline level. This is indicated by a fall in the HRF. This process is illustrated in the graph below. The values on the vertical axis are not of concern as for now.

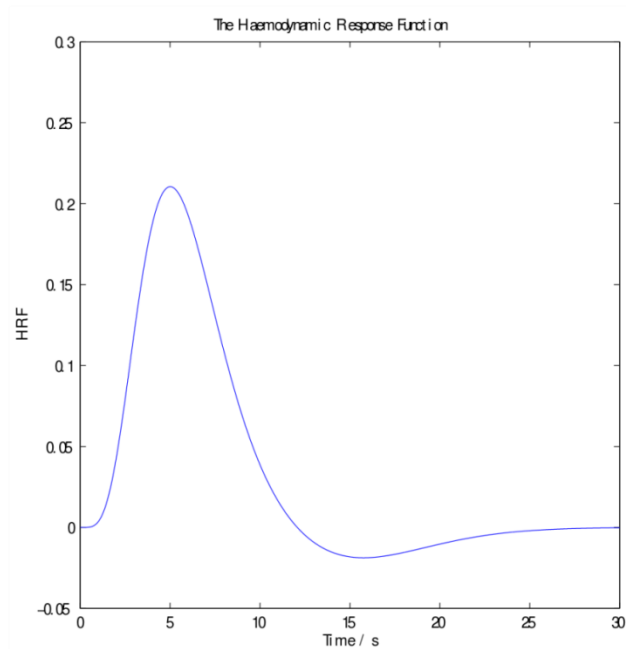


*Fig. 1 A typical hemodynamic response function (HRF).*

As discussed, the hemodynamic response is in fact a response to the neuronal activation in the brain, which is why it is an effective means of brain mapping. That is, by measuring the HRF, it can be clarified which part of the human brain controls which part of the body. But how is HRF measured?

The answer is functional magnetic resonance imaging (fMRI). MRI is a medical imaging technique that utilizes strong magnetic fields, magnetic field gradients and radio waves to generate images of the organs in the body. fMRI is a means of monitoring brain activity by detecting changes associated with cerebral blood flow (CBF). CBF is the blood supply to the brain in a given period of time, which delivers oxygen to the brain tissue. The oxygen content of the brain causes distortions in the local magnetic resonance (MR) signal, providing a method for detecting brain activation.

Hemoglobin (Hb), the means of oxygen transport in the red blood cells, is diamagnetic when oxygenated (that is when it contains oxygen) and paramagnetic when deoxygenated (that is when it contains no oxygen). Following increased neural activity in the brain, the local CBF increases much more than the cerebral metabolic rate of oxygen (CMRO<sub>2</sub>), that is the rate at which the

brain consumes the oxygen. Thus, decreasing the amount of deoxygenated Hb in the brain which is defined by a cerebral oxygen extraction fraction, E.

$$E = \frac{\text{oxygen consumption}}{\text{oxygen delivery}} = \frac{CMRO_2}{C_a \cdot CBF} \quad (1)$$

where  $C_a$  is the oxygen content of blood. Hence, as a result of activation, E decreases and the local blood is more oxygenated and consequently more diamagnetic. This means less alteration in the local magnetic susceptibility and the magnetic field distortions are reduced, resulting in a slightly stronger local MR signal. For this reason, this signal is called the blood oxygenation level dependent (BOLD) signal. This small BOLD signal change is the mapping signal used in most functional magnetic resonance imaging (fMRI) applications.

However, the BOLD signal does not directly measure the neuronal activity itself. Instead, the BOLD effect is sensitive to the changes in CBF,  $CMRO_2$ , and cerebral blood volume (CBV), which is the instantaneous amount of blood in the brain's vascular system. This set of physiological responses is referred to collectively as the hemodynamic response to activation. A critical goal for interpreting fMRI data is to understand the underlying link between neuronal activity and the hemodynamic response.

Our goal is to develop a mathematical description of the translation from an applied stimulus pattern to the measured BOLD signal. A quantitative working model such as this can guide experimental design and inform the interpretation of experimental results. In particular, a modeling approach can help to identify possible sources of variability of the BOLD response across the brain and across subject populations, and provide mechanisms for how such variability can arise despite similar underlying neural responses.

## **Mathematical model**

In the following discussion of models of the hemodynamic response, we will assume that the measurable quantities are time series of CBF and BOLD, and that under some circumstances CBV can be measured as well. Four models are considered, which when combined provide a model of the full path from a temporal stimulus pattern to a measured CBF response and a

BOLD response. The models treat (1) the BOLD signal as a function of changes in E and CBV; (2) the balloon model, proposed to describe the transient dynamics of CBV and deoxyhemoglobin and how they affect the BOLD signal; (3) neurovascular coupling, relating the responses in CBF and  $CMRO_2$  to the neural activity response; and (4) a simple model for the temporal nonlinearity of the neural response itself. Recent experimental findings on the linearity of the BOLD response and the effect of the baseline physiological state on the BOLD response are considered in light of these models.

### **Experimental characterization of the hemodynamic response**

Based on numerous experimental studies of the BOLD and CBF responses to brain activation, the following are the key findings that motivate the modeling:

1. CBF increases much more than  $CMRO_2$  with brain activation, reducing E and the total deoxyhemoglobin present in an image voxel. This phenomenon is the primary cause of the BOLD signal change.
2. The CBF and BOLD responses to even a very brief stimulus are delayed by 1–2 s and have a temporal width on the order of 4–6 s. For a sustained stimulus of 20 s or longer, the response typically reaches a plateau value, although there can be substantial variation (e.g., an initial overshoot, a slow ramp, or an overshoot at the end of the stimulus).
3. A post-stimulus undershoot of the BOLD signal is common and may last for 30 s or more, with longer duration stimuli tending to have longer post-undershoots. The CBF response typically shows only a shorter and weaker post-stimulus undershoot, or none at all.
4. Some investigators have reported an initial dip of the BOLD signal lasting 1–2 s before the standard BOLD signal increase, and a corresponding transient increase of deoxyhemoglobin has been reported in optical imaging studies. The effect is small and not always present, but it has stirred interest because it may reflect a rapid increase of  $CMRO_2$  before the CBF increase, and this phenomenon may be better localized to the area of increased metabolism (i.e., the CBF increase may cover a wider area).
5. The BOLD response typically exhibits a temporal nonlinearity such that an appropriately shifted and added response to a brief stimulus over-predicts the true response to an extended

stimulus. This temporal nonlinearity is most pronounced when the brief stimulus is less than about 4 s and the extended stimulus is longer than 6 s. Comparing short and long duration stimuli that are both longer than about 4 s, the temporal nonlinearity is reduced.

6. Nonlinearity has also been reported as a “refractory period”, such that two identical stimuli presented close together in time produce a net response with less than twice the integrated response of a single stimulus alone.

7. There is a growing body of evidence suggesting that the baseline CBF can have a strong effect on the magnitude of the BOLD response to the same stimulus. For example, if baseline CBF is increased by breathing CO<sub>2</sub>, the BOLD response to the same task is reduced substantially. Interestingly, however, the CBF change ( $\Delta$ CBF) appears to remain the same despite the baseline change.

With these examples as experimental background, we now consider quantitative models for the hemodynamic response.

### **Definition of dynamic variables**

The dynamic variables and parameters utilized in the description of the model are summarized in Tabel 1. The assumed causal connections between the variables are diagrammed in Figure 1: (1) the stimulus pattern  $s(t)$  drives the neural response  $N(t)$ ; (2)  $N(t)$  drives the CBF response  $f(t)$  and the CMRO<sub>2</sub> response  $m(t)$ ; (3)  $f(t)$  and  $m(t)$  drive the balloon model to produce the CBV response  $v(t)$  and the total deoxyhemoglobin response  $q(t)$ ; and (4)  $q(t)$  and  $v(t)$  combine to produce the BOLD signal. In most cases we use the convention that upper case variables refer to absolute quantities, while lower case variables are the same quantity normalized to its baseline value. Then, for example, at baseline  $f = m = q = v = 1$  and  $E = E_0$ .

For the calculations shown here, we are particularly interested in transient features and nonlinearities of the BOLD response. To emphasize these effects, we assume simple forms for scaling the stimulus and the neural response. The stimulus is considered to be a brief event (e.g., one reversal of a visually presented checkerboard), and these events can be presented in any pattern, including direct concatenation to produce a sustained stimulus (e.g., a flickering checkerboard). The stimulus pattern  $s(t)$  is then a time series of ones and zeroes defining when

events occurred. The neural response is defined such that  $N(t) = 1$  on the plateau of a sustained stimulus when no adaptation effects are operating.

*Table 1 Model variables, parameters and typical values.*

	Definitions
<i>Dynamic variables</i>	
$f(t)$	CBF normalized to baseline
$m(t)$	CMRO <sub>2</sub> normalized to baseline
$v(t)$	CBV normalized to baseline
$q(t)$	DeoxyHb content normalized to baseline
$b(t)$	BOLD signal change (%)
$E(t)$	O <sub>2</sub> extraction fraction
$N(t)$	Neural activity
$s(t)$	Stimulus pattern
<i>Physiological Parameters</i>	
$F_0$ (0.01 s <sup>-1</sup> )	Baseline CBF (0.01 s <sup>-1</sup> = 60 ml.min <sup>-1</sup> .ml <sup>-1</sup> tissue)
$\Delta F$	Absolute CBF change with activation
$E_0$ (0.4)	Baseline O <sub>2</sub> extraction fraction
$V_0$ (0.03)	Baseline blood volume
$\alpha$ (0.4)	Steady state flow-volume relation $v = f^\alpha$
$n$ (2-3)	Steady state flow-metabolism relation $n = (f-1)(m-1)$
<i>BOLD signal parameters</i>	
$a_1$ (3.4)	Weight for deoxyHb change
$a_2$ (1.0)	Weight for blood volume change
<i>Balloon model parameters</i>	
$f_{out}(v,t)$	Outflow from the balloon (transiently different from $f$ )



$\tau_{MTT}$	Transit time through the balloon ( $V_0/F_0$ )
$\tau_+$ (0-30s)	Viscoelastic time constant (inflation)
$\tau_-$ (0-30s)	Viscoelastic time constant (deflation)
<i>Neural response parameters</i>	
$\kappa_n$ (0.0-2.0)	Inhibitory gain factor
$\tau_i$ (1-3s)	Inhibitory time constant
<i>Neurovascular coupling (assumed linear)</i>	
$\tau_f$ (4s)	Width of CBF impulse response
$\tau_m$ (4s)	Width of CMRO <sub>2</sub> impulse response
$\delta t$ (0-2s)	Delay of CBF relative to CMRO <sub>2</sub> responses
$f_i$ (1.0-2.0)	Normalized CBF response to sustained neural activation

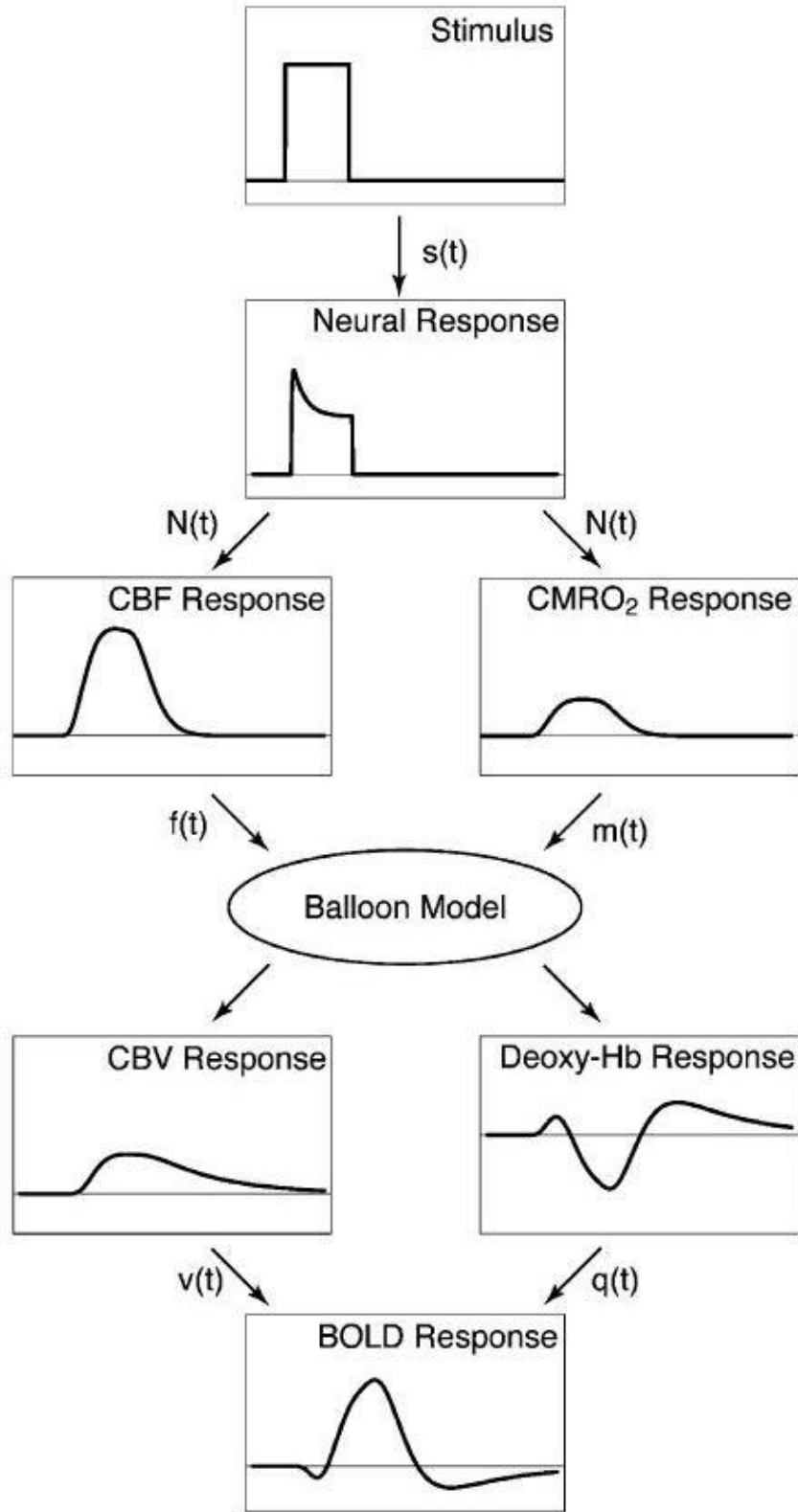


*Fig. 2 Diagram of the proposed model linking the applied stimulus to the resulting physiological responses and the measured BOLD response*

## Physiological relationships

The CBF increase associated with neural activity is triggered by a relaxation of the smooth muscle in the wall of the arterioles. The arterioles provide most of the resistance in the vascular tree and provide a way to quickly decrease vascular resistance by relaxing. As the resistance of the arterioles decreases, the pressure drop across these vessels also decreases, raising the pressure in the capillaries and veins. These vessels may also expand due to the increased pressure, further increasing the CBV. Experimental studies (Grubb et al., 1974) have indicated that the steady-state relationship between CBF and CBV can be described with a power law:

$$V = f^\alpha \quad (2)$$

where the exponent is approximately  $\alpha = 0.4$ . This empirical relationship applies to the entire blood volume. For our purposes we are merely interested in the venous volume, and to a lesser extent the capillary volume, because this is where the deoxyhemoglobin lies. Nevertheless, a value of  $\alpha = 0.4$  is often used in modeling the BOLD effect.

At steady-state, CBF and  $CMRO_2$  are related to each other by the arterial oxygen concentration  $C_a$  and the net oxygen extraction fraction  $E$ :

$$CMRO_2 = E \cdot C_a \cdot CBF \quad (3)$$

$$m = \frac{E}{E_0} f$$

The local oxygenation of the venous blood depends directly on  $E$ .

For modest changes around an awake baseline state, experiments suggest that the relationship between the CBF and  $CMRO_2$  changes can be characterized as linear with a slope  $n$  defined as the fractional change in CBF divided by the fractional change in  $CMRO_2$ :

$$n = \frac{\Delta CBF / CBF_0}{\Delta CMRO_2 / CMRO_{20}} \quad (4)$$

$$n = \frac{f - 1}{m - 1}$$

where the subscript "0" denotes baseline values. Experimental measurements find  $n = 2-3$ .

The fact that  $n > 1$ , so that  $E$  decreases with activation, is the physiological source of the BOLD effect.

Equations (2)-(4) are useful for relating the key physiological quantities involved in the BOLD effect, but it is important to remember that while equation (3) is necessarily true from the definition of the terms involved, equations (2) and (4) are empirical relationships, and the uniformity of these relationships across brain regions, subject populations, species, and different physiological states is still open to question and in need of experimental evaluation.

### **Modeling the BOLD effect**

The BOLD effect is primarily due to changes in local deoxyhemoglobin content, but quantitative modeling of this effect requires some subtlety. In fact, there are two sources of signal change that must be modeled: the intravascular and the extravascular signals. Both regimes are affected by the magnetic field gradients created by the presence of deoxyhemoglobin, which cause the MR signal to decay faster when deoxyhemoglobin increases. Although the intrinsic intravascular signal is much less than the extravascular signal, the sensitivity of the intravascular signal to the oxygenation of blood is much greater. The result is that the intravascular contribution likely accounts for half or more of the signal change. The total deoxyhemoglobin content could change either by changing the oxygen extraction fraction or by changing the volume of the venous blood, so the role of volume changes must be included. And finally, for the smallest vessels, diffusion effects can be important. Thus modeling the BOLD effect depends not only on the biophysical models for how intravascular susceptibility differences alter the signal, but also physiological models for how CBF, CBV, and CMRO<sub>2</sub> change with activation. The relative changes in CBF and CMRO<sub>2</sub> determine the level of oxygenation of the blood, and the CBV determines the total amount of blood (and thus the total deoxyhemoglobin present in the voxel).

### **Magnetic susceptibility effects and the MR signal**

The MR signal for a typical gradient echo acquisition (an MR imaging technique) is modeled as a simple exponential dependence on the echo time TE and can be written as:

$$S = S_{\max} \cdot e^{-TE \cdot R_2^*} \quad (5)$$

$$R_2^* = R_2^*(0) + R$$

where  $S_{max}$  is the effective spin density (the signal that would be measured if TE could be reduced to zero). The transverse relaxation rate constant  $R_2^*$  is written as a sum of two terms:  $R_2^*(0)$  is the value of  $R_2^*$  if no deoxyhemoglobin is present, and  $R$  describes the additional relaxation produced by deoxyhemoglobin. Note that typically  $R_2^*(0)$  is much larger than  $R$ , that is, the local  $T_2^*$  that describes the decay of the signal is largely determined by the intrinsic  $T_2$  and large-scale field gradients through the voxel, and the additional effect of deoxyhemoglobin is minor. For this reason, the signal changes due to the BOLD effect are small, but measurable.

We now assume that with activation  $R$  is the only parameter that changes. Using the subscript “0” to denote the resting value and “act” to denote the activated value, the BOLD signal change with activation  $\Delta S = S_{act} - S_0$  is:

$$\frac{\Delta S}{S_0} = e^{-\Delta R_2^* \cdot TE} - 1 \approx \Delta R_2^* \cdot TE \quad (6)$$

$$\Delta R_2^* = R_{act} - R_0$$

The key question is: how does  $\Delta R_2^*$  depend on blood oxygenation and volume? The magnitude of the magnetic field distortions near a magnetized vessel is proportional to the magnetic susceptibility difference between the blood and the surrounding extravascular space. Experiments indicate that the magnetic susceptibility difference can be accurately modeled as having a linear dependence on the local deoxyhemoglobin concentration in blood, and this quantity in turn can be expressed in terms of the change in the oxygen extraction fraction E. In literature a power law is assumed between R and  $\Delta B$ , the magnitude of the field distortions:  $R \propto \Delta B^\beta$ .

In addition to the change in E with activation, a change in blood volume also affects R. For example, even if the oxygenation of the blood did not change but the venous blood volume increased, the total deoxyhemoglobin would be increased, and we would expect this to increase R and decrease the net MR signal. Numerical simulations suggest that a reasonable approximation is to assume that R is proportional to V, the venous blood volume. Combining these dependences, the contribution of deoxyhemoglobin to the relaxation rate is modeled as:

$$R \propto VE^\beta$$

(7)

### The BOLD signal change

The ideas in the previous section can be combined to model the MR signal in terms of the blood volume ( $V$ ) and the oxygen extraction fraction ( $E$ ):

$$\frac{\Delta S}{S_0} \approx A \cdot \left[ 1 - \frac{V_{act}}{V_0} \left( \frac{E_{act}}{E_0} \right)^\beta \right] \quad (8)$$

The parameter  $A$  lumps together  $TE$  and the unknown proportionality constant in equation (7), and is also proportional to the local resting blood volume  $V_0$  and the resting oxygen extraction fraction  $E_0^\beta$ . A decrease of either of the physiological quantities ( $V$  or  $E$ ) will decrease the local deoxyhemoglobin concentration and so increase the MR signal.

Equation (8) for the BOLD signal change is quite simple, depending on two physiological changes (the change in blood volume  $V$  and oxygen extraction fraction  $E$ ) and two additional parameters  $\beta$  and  $A$ . The form of the signal equation directly describes the ceiling effect on the BOLD signal. In simple terms,  $A$  is the maximum BOLD signal change that could occur, corresponding to complete removal of deoxyhemoglobin from the voxel. The parameter  $b$  should be primarily field dependent, and we can assume that it is not a function of brain region. The parameter  $A$ , however, is a local parameter and so may vary across different voxels in the brain. Note that this parameter is proportional to the value of  $R$  at rest, the relaxation rate produced by deoxyhemoglobin in the baseline state. This means that the more deoxyhemoglobin is present at rest, the larger the BOLD signal change will be for the same fractional change in  $V$  and  $E$  with activation. We will come back to this later when we consider the effect of the baseline condition on the magnitude of the BOLD effect.

In our notation with dynamic variables normalized to their baseline values, and assuming equation (2) is accurate, the basic BOLD signal equation is:

$$\frac{\Delta S}{S_0} = A \cdot \left( 1 - f^{\alpha-\beta} m^\beta \right)$$

(9)

Although equation (9) is a very useful model, the reader should bear in mind that it does not necessarily describe all of the effects that may contribute to the measured signal change in an activation experiment. Specifically, small direct effects of CBF and CBV changes on the MR signal that are independent of the BOLD effect are likely present in real data. For example, if the repetition time TR is shorter than the  $T_1$  of blood and the flip angle is large (e.g.,  $90^\circ$ ), the increased delivery of fresh unsaturated blood due to increased CBF could increase the net signal slightly. In addition, the intrinsic signal from arterial blood typically is larger than the intrinsic signal of the extravascular space, so increasing the arterial blood volume fraction of the voxel could also produce a slight signal increase. Note that both of these effects are due to arterial blood changes, where deoxyhemoglobin is negligible, so these are effects in addition to the BOLD effect. In most applications, these effects are thought to be small compared to the BOLD effect, especially at higher magnetic fields, but they may not be negligible.

### **Alternative forms for the BOLD signal model**

An alternate form of the BOLD signal equation was proposed to model the dynamics of the BOLD effect in the context of the balloon model (described in the next section). The derivation of this model is based on separate estimates of the intravascular and extravascular signal changes. In this way, the model can be used to analyze experiments in which flow-nulling bipolar gradient pulses are applied to destroy the signal of moving blood, and thus eliminate the intravascular signal changes from the BOLD effect. The key physiological variables are the total deoxyhemoglobin ( $q$ ) and the blood volume ( $v$ ), both normalized to their values at rest. In this model, the BOLD signal change is written as:

$$\frac{\Delta S}{S} \approx V_0 [a_1(1-q) - a_2(1-v)] \quad (10)$$

where  $V_0$  is the resting venous blood volume fraction (e.g., 0.03) and the dimensionless parameters  $a_1$  and  $a_2$  depend on several experimental and physiological parameters.

Equations (9) and (10) are framed in terms of different variables, but they are approximately equivalent expressions for the BOLD signal change. Equation (9) is useful for calibrated BOLD studies, because it explicitly includes CBF, a measurable quantity. On the other hand, equation (10) deals explicitly with the variables of the balloon model.

## The balloon model

The balloon model was motivated by the observation in an animal study that CBV returned to baseline more slowly than CBF after the end of the stimulus and the idea that this effect might explain the post stimulus undershoot of the BOLD signal that is often observed. The balloon model has been refined and compared with experimental data and some errors in the original parameter estimates were recently corrected. The model is capable of producing BOLD post stimulus undershoots that match well with experimental data. However, the central premise of the model, that the undershoot occurs when CBV returns slowly to baseline, has not been definitively established and focused experimental tests of this question are needed.

The central idea of the model is that the venous compartment is treated as a distensible balloon. The inflow to the balloon  $f_{in}$  is the cerebral blood flow ( $f$  in our current notation), while the outflow from the balloon  $f_{out}$  is an increasing function of the balloon volume. The two dynamical variables are the total deoxyhemoglobin  $q(t)$  and the volume of the balloon  $v(t)$ . The equations of the balloon model represent mass conservation for blood and deoxyhemoglobin as they pass through the venous balloon:

$$\frac{dq}{dt} = \frac{1}{\tau_{MTT}} \left[ f(t) \frac{E(t)}{E_0} - \frac{q(t)}{v(t)} f_{out}(v,t) \right] \quad (11)$$

$$\frac{dv}{dt} = \frac{1}{\tau_{MTT}} [f(t) - f_{out}(v,t)]$$

The net extraction fraction of oxygen is  $E(t)$ , and the resting value is typically  $E_0 = 0.4$ . The time dimension of the equations is scaled by the time constant  $\tau_{MTT}$ , the mean transit time through the balloon at rest. For a cerebral blood flow of  $60 \text{ ml min}^{-1} 100 \text{ ml}^{-1}$  of tissue (equivalent to a rate constant of  $0.01 \text{ s}^{-1}$ ) and a resting venous blood volume fraction of  $V_0 = 0.03$ , the mean transit time is  $\tau_{MTT} = 3 \text{ s}$ .

The driving function of the system is the quantity  $f(t)E(t)$ . Note that the quantity  $fE/E_0$  is simply the cerebral metabolic rate of oxygen (CMRO<sub>2</sub>) normalized to its value at rest ( $m$ ).

The model proposed for the outflow, is one that takes into account the viscoelastic effects of the blood which cause the blood volume to transiently lag behind the steady state relationship



between CBF and total blood volume described by equation (2). In this model  $f_{out}$  is treated as a function of the balloon volume and the rate of change of that volume:

$$f_{out}(v) = v^a + \tau \frac{dv}{dt} \quad (12)$$

With this form, the balloon initially resists a change in volume, but eventually settles into a new steady-state that conforms to the power law model in equation (2). The time constant  $\tau$  controls how long this transient adjustment requires. A nonzero value for  $\tau$  produces hysteresis in the curve  $f_{out}(v)$ , so that the system follows a different curve on inflation and deflation. To generalize this form and enable more fine tuning to data, we allow  $\tau$  to take on different values during inflation ( $\tau_+$ ) and deflation ( $\tau_-$ ).

For a specified driving function  $f(t)E(t)$ , and values for the parameters  $\tau_{MTT}$ ,  $E_0$ ,  $a$ ,  $\tau_+$ , and  $\tau_-$ , equations (11) and (12) can be integrated numerically to yield dynamic time courses for  $q(t)$  and  $v(t)$ . These dynamic physiological quantities can then be combined with the BOLD signal model (equation (10)) to generate MR signal curves. Figure 3 shows balloon model curves for a simple smooth trapezoidal form for  $f(t)$  and a fixed CBF/CMRO<sub>2</sub> coupling parameter  $n = 3$ . A nonzero value for  $\tau_+$  creates an initial overshoot of the BOLD signal and a nonzero value for  $\tau_-$  creates a post stimulus undershoot. These curves show that quite different BOLD responses can result from the same underlying CBF and CMRO<sub>2</sub> response.

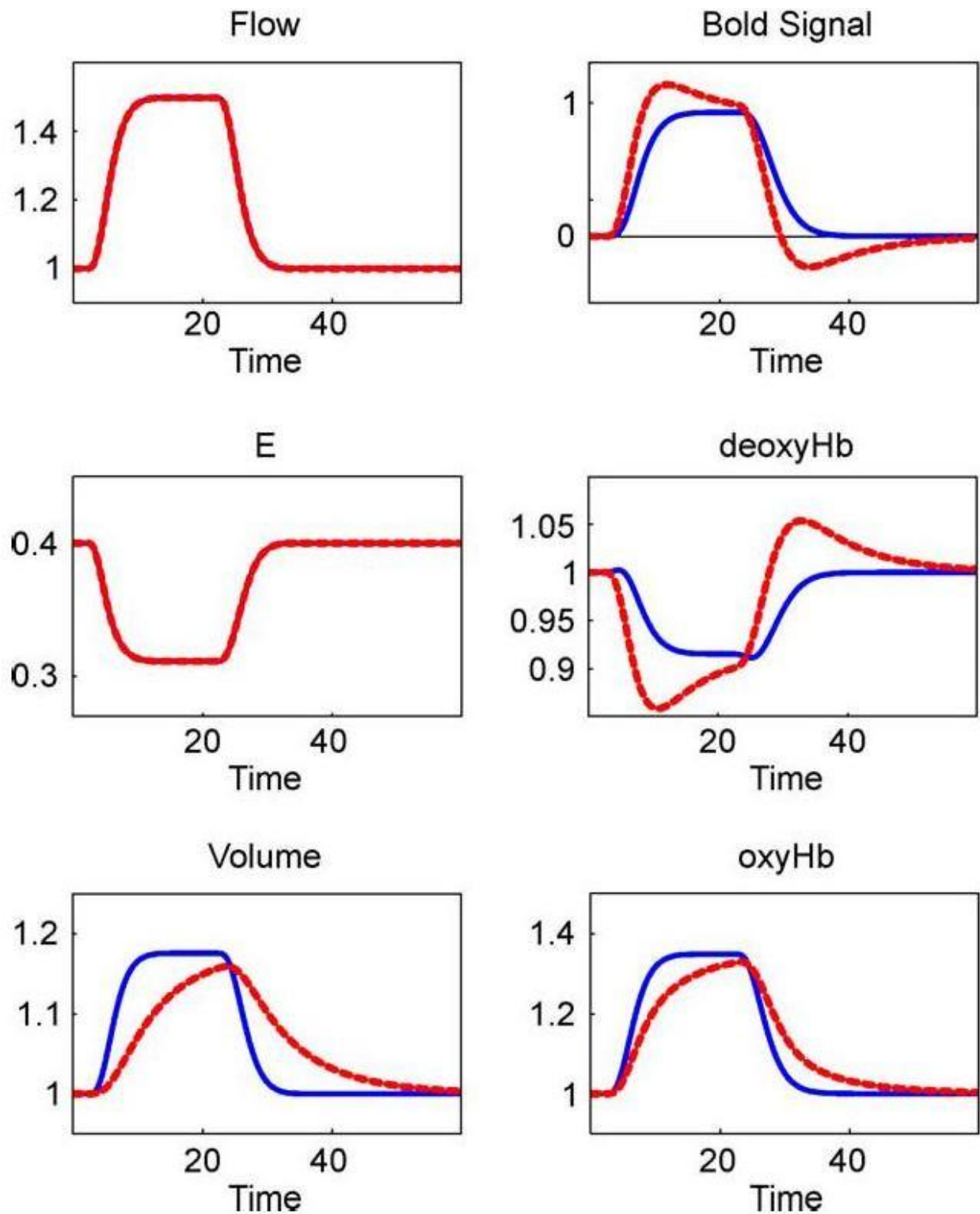


*Fig. 3 Dynamic curves calculated with the balloon model for two sets of model parameters:  $\tau_+ = \tau_- = 0$  (blue solid curve) and  $\tau_+ = \tau_- = 20$  (red dashed curve). The input curves for inflow  $f(t)$  ("Flow") and oxygen extraction fraction ("E") were identical for both calculations. Nonzero values for  $\tau_+$  or  $\tau_-$  create an initial overshoot or post stimulus undershoot of the BOLD signal, respectively, by causing the CBV to change more slowly than CBF.*

## Neurovascular coupling

We do not currently have a quantitative understanding of the mechanisms that couple neural activity to CBF and CMRO<sub>2</sub> changes. In fact, there is no consensus on exactly which aspect of neural activity drives the hemodynamic response, and this is an active area of research. Experimental studies comparing electrophysiological measurements with BOLD and CBF changes have found that the hemodynamic responses correlate better with local mean field potential, rather than local spiking rates, suggesting that the hemodynamic response is dominantly driven by input synaptic activity rather than output spiking activity. Theoretical analyses of the energy budget for neuronal signaling provide some support for this picture as well. Finally, there is some evidence that inhibitory activity does not elicit a measurable BOLD response.

One of the goals of modeling the hemodynamic response is to understand the origins of the nonlinearities of the response, and for that purpose, it is useful to have a model that includes a nonlinear transformation from the stimulus pattern  $s(t)$  to the CBF response  $f(t)$ . Such a nonlinearity could arise in the step from  $s(t)$  to the neural response  $N(t)$ , as, for example, in adaptation. In addition, the step from neural activity to CBF response could be nonlinear, for example, through a ceiling effect on CBF change. Given our poor understanding of the mechanisms of neurovascular coupling, we take here a simple approach and assume that the nonlinear step is entirely in the transformation from  $s(t)$  to  $N(t)$ , and in the next section we introduce a simple model for this process that includes adaptation. We then assume that both CBF and CMRO<sub>2</sub> are linear convolutions of an impulse response function  $h(t)$  with the appropriate measure of neural activity  $N(t)$ .

A plausible shape for  $h(t)$  is a gamma-variate function with a full width at half maximum (FWHM) of about 4 s. For the calculations here we use the form:

$$h(t) = \frac{1}{k\tau_h(k-1)!} \left( \frac{t}{\tau_h} \right)^{k-1} e^{-t/\tau_h} \quad (13)$$

with  $k = 3$ . To model the observed lag of the hemodynamic response we also add a delay of this response (typically about 1 s) in the calculations.

The shape  $h(t)$  is then scaled to provide the desired amplitude and duration of the impulse response. For this shape, and a desired FWHM of  $\tau_f$ , the time constant in equation (13) is given by the empirical expression  $\tau_f = 0.242 \tau_f$ . The CBF and CMRO<sub>2</sub> responses to activation are then:

$$f(t) = 1 + (f_l - 1)h(t - \delta t_f) * N(t) \quad (14)$$

$$m(t) = 1 + (m_l - 1)g(t - \delta t_m) * N(t)$$

The symbol \* denotes convolution. The parameter  $f_l$  scales the response shape to the appropriate amplitude and represents the normalized flow increase on the plateau of the CBF response to a sustained neural activity with unit amplitude. For example, if  $N(t)$  is a 30-s block with amplitude 1, and the model parameters are  $f_l = 1.5$  and  $\tau_f = 4$  s, the CBF response is a smoothed version of the block due to the 4-s-wide smoothing kernel, and on the plateau CBF is increased by 50%. The parameter  $\delta t_f$  is the delay after the start of the stimulus before the CBF response begins.

We model the CMRO<sub>2</sub> response in equation (14) as an independent convolution with potentially independent amplitude, width, and delay defined by  $g(t)$ . In the calculations here, we assume a coupled response such that the amplitude of the CMRO<sub>2</sub> impulse response is given by  $(m_l - 1) = (f_l - 1)/n$ , and the width is the same. In this way the steady-state response is constrained to follow the empirical physiological relationship in equation (4). However, by introducing a delay  $\delta t = \delta t_f - \delta t_m$  of the CBF response relative to the CMRO<sub>2</sub> response, we can introduce interesting dynamics such as an initial dip of the BOLD response. This approach is analogous to the balloon model, where the model is constrained to follow the physiological relationship in equation (2) at steady state, but allows substantial range for transient responses.

Figure 4 illustrates the type of transient features that can result from combining the balloon model with the independent convolution model. The figure shows different dynamic responses of CBF, CMRO<sub>2</sub>, and CBV to the same 20-s uniform block of neural activity. In these calculations, the responses  $f(t)$  and  $m(t)$  calculated from the independent convolutions were used as input to the balloon model to calculate  $v(t)$  and  $q(t)$ . The first panel shows the response when the viscoelastic time constants of the balloon model are zero, and there is no delay between  $f(t)$  and  $m(t)$ . In the second panel,  $\tau_v$  was increased to 20 s, and in the third panel the impulse response for CBF was delayed by  $\delta t = 1$  s relative to the CMRO<sub>2</sub> response. The BOLD response for the last combination shows both an initial dip and a post stimulus undershoot. The physiological

dynamics is also shown as a trajectory in the  $q/v$  plane on the right side of figure 4, and the BOLD signal is a one-dimensional projection of this two dimensional trajectory.

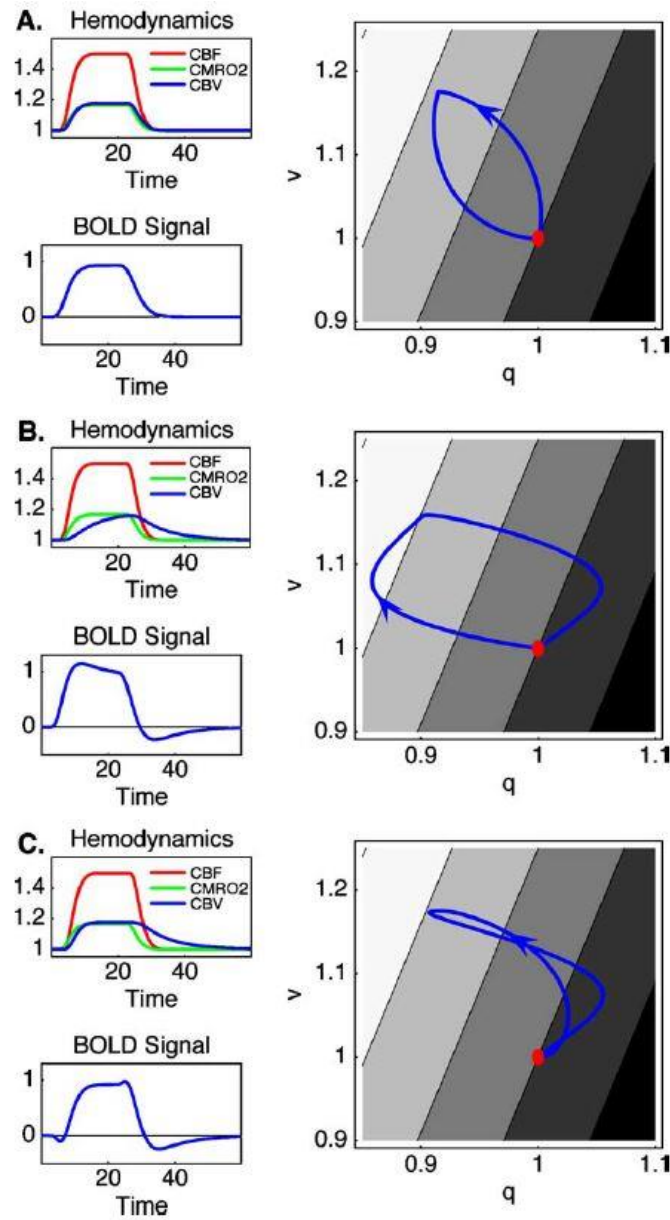


*Fig. 4 Transients of the BOLD response due to variations in the timing of the responses of the physiological variables CBF, CBV, and CMRO<sub>2</sub>. These variables and the resulting BOLD response are shown on the left. The BOLD response is diagrammed on the right as a trajectory in the  $q/v$  plane, where  $q$  is the total deoxyhemoglobin and  $v$  is the blood volume, both normalized to their baseline values (indicated by a red dot). The BOLD signal intensity is shown as a shaded contour plot in the  $q/v$  plane based on Eq. (9). The three sets of figures illustrate: (A) a simple BOLD response in which the physiological changes have similar time courses; (B) a BOLD response with an initial overshoot and post stimulus undershoot due to a slow CBV response ( $s_+ =$*

*s*

*= 20 s); and (C) a BOLD response with an initial dip as well, created by adding a 1-s delay of the CBF impulse response relative to the CMRO<sub>2</sub> impulse response.*

## Modeling the neural response

As discussed in the previous section, the approach we have adopted is to model the CBF and CMRO<sub>2</sub> responses as linear convolutions with the neural activity  $N(t)$ , and uses a model for the step from the stimulus  $s(t)$  to  $N(t)$  that includes the possibility for adaptation. We chose a simple inhibitory feedback system, in which the neural response  $N(t)$  is treated as the difference between an excitatory input  $s(t)$  and an inhibitory input  $I(t)$ . The inhibitory input  $I(t)$  is driven by the neural response  $N(t)$  with a gain factor  $\kappa$  and a time constant  $\tau_I$ . The set of equations is then:

$$N(t) = s(t) - I(t) \quad (14)$$

$$\frac{dI}{dt} = \frac{\kappa N(t) - I(t)}{\tau_I}$$

From these equations, the neural response to a sustained stimulus is an initial peak followed by decay to a lower plateau level, with the difference between the peak and plateau values determined by  $\kappa$ . As written, these equations are linear, and the initial peak of the response would be balanced by a dip after the end of the stimulus, and such a post undershoot of the neural response has been observed. We introduce a nonlinear component, as well as the possibility of a post-stimulus neural undershoot, by introducing a baseline neural activity  $N_0$  and the requirement that the neural response is a positive quantity (i.e., if the calculated quantity  $N_0 + N(t) < 0$ , it is replaced by zero). Then if the resting stimulus level is  $N_0 = 0$ , there is no dip following the end of the stimulus. This is the adaptation pattern originally proposed to describe the observed nonlinearities of the BOLD response in the visual cortex. On the other hand, if  $N_0 > 0$ , there will be a post-stimulus undershoot of the neural response. In addition to diminishing the response to a sustained stimulus, this model also introduces a “refractory” effect. If two events

are presented close together (within  $\tau_i$  of each other), then the net response to both events will have less than twice the area of the response to a single event.

This model provides a simple form for introducing a nonlinearity that can be applied to any stimulus pattern: the amplitude of this nonlinear effect is governed by  $\kappa$  and the duration of the “refractory” period is determined by  $\tau_i$ . Figure 5 shows an example that includes both a two-pulse inhibition experiment and a sustained stimulus.

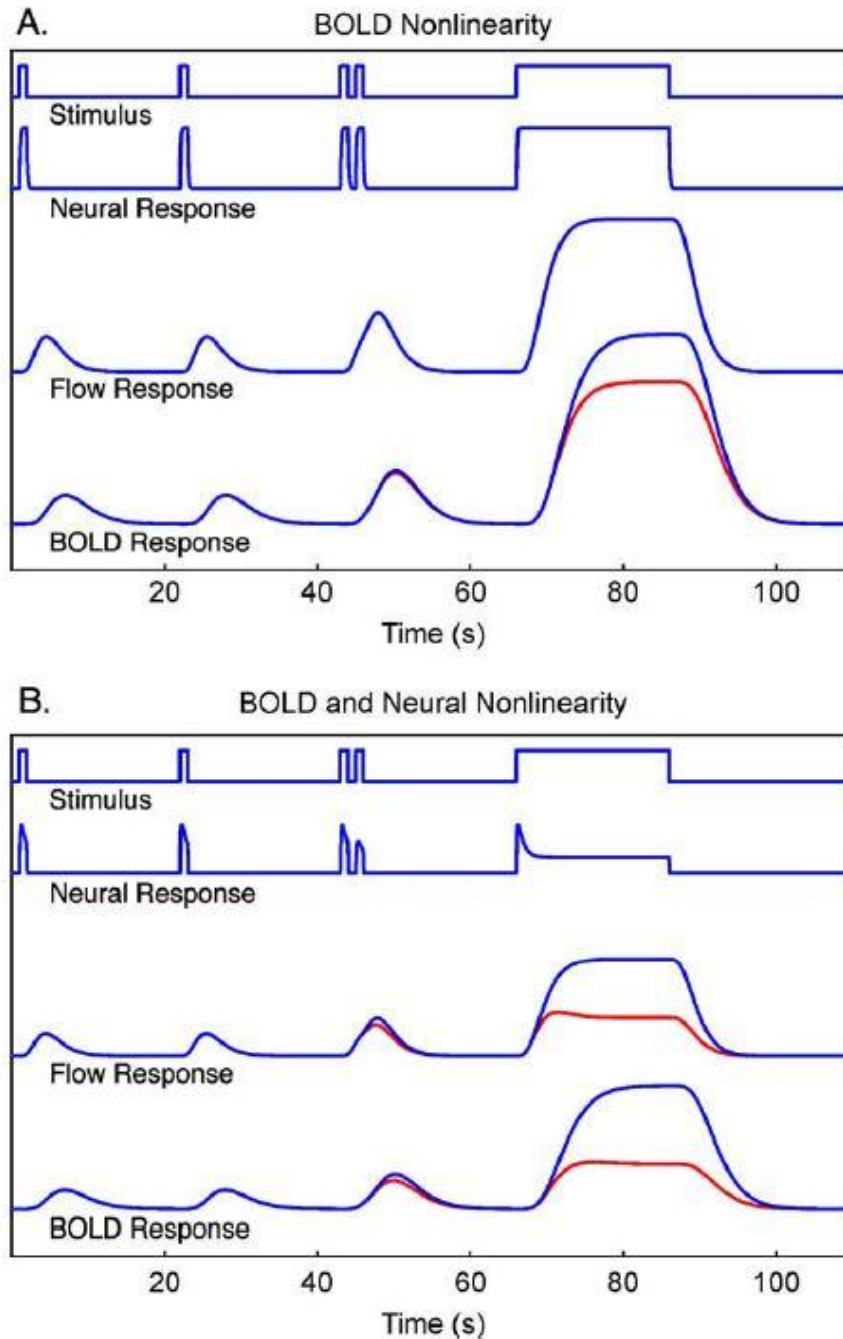


*Fig. 5 Nonlinearity of the BOLD response with respect to additivity of overlapped responses. A single event with a 1-s duration (the first stimulus shown) was used to predict the response to a second identical event presented 20 s later, a pair of identical events separated by a 1-s interstimulus interval, and a block of 20 identical events concatenated to create a continuous stimulation. For the flow and BOLD responses, the predicted curve is shown in blue and the actual calculated curve is shown in red. The calculations show two sources of nonlinearity: (A) with a purely linear neural ( $j = 0$ ) and flow response, the BOLD response still shows a pronounced nonlinearity in the prediction of a sustained response due to the BOLD ceiling effect, with the area of the actual response 22% lower than the linear prediction. In addition, the area under the response to two pulses close together is slightly reduced by 4% from twice the area under the response to a single pulse. (B) With a neural response nonlinearity as well ( $j = 3$  and  $sI = 3$  s), both the flow and BOLD responses exhibit overprediction of the response to a sustained stimulus and a more pronounced “refractory period” in the two pulse experiment (area of the response reduced by 17%).*



## Summary

We have constructed a proposed mathematical framework to link an applied stimulus pattern with the resulting BOLD response. The stimulus pattern drives the neural response, which could exhibit adaptation effects controlled by the parameters  $\kappa$  and  $\tau_i$ . The neural response independently drives the CBF and CMRO<sub>2</sub> responses, treated as simple linear convolutions. The amplitudes of these two responses are defined in terms of a flow amplitude  $f_l$  and a steady-state CBF/CMRO<sub>2</sub> coupling parameter  $n$ . A slight delay of the CBF response relative to the CMRO<sub>2</sub> response creates an initial dip in the BOLD response. The CBF and CMRO<sub>2</sub> response drives the balloon model, which determines the time course of CBV and total deoxyhemoglobin. Key parameters for the balloon model are the resting O<sub>2</sub> extraction fraction  $E_0$  and two viscoelastic time constants  $\tau_+$  and  $\tau_-$ . When these time constants are nonzero, the BOLD response exhibits an initial overshoot and a post stimulus undershoot that are not present in the CBF response. Finally, the deoxyhemoglobin and CBV responses determine the dynamic BOLD response, with the amplitude scaled by the resting venous blood volume fraction  $V_0$ .

## References

- [1] Buxton, Richard B., et al. "Modeling the hemodynamic response to brain activation." *Neuroimage* 23 (2004): S220-S233.
- [2] Deneux, Thomas, and Olivier Faugeras. "Using nonlinear models in fMRI data analysis: model selection and activation detection." *NeuroImage* 32.4 (2006): 1669-1689.
- [3] Friston, Karl J., et al. "Event-related fMRI: characterizing differential responses." *Neuroimage* 7.1 (1998): 30-40.
- [4] Friston, Karl J., et al. "Nonlinear responses in fMRI: the Balloon model, Volterra kernels, and other hemodynamics." *NeuroImage* 12.4 (2000): 466-477.
- [5] Friston, Karl J. "Bayesian estimation of dynamical systems: an application to fMRI." *NeuroImage* 16.2 (2002): 513-530.
- [6] Handwerker, Daniel A., et al. "The continuing challenge of understanding and modeling hemodynamic variation in fMRI." *Neuroimage* 62.2 (2012): 1017-1023.
- [7] Lindquist, Martin A., et al. "Modeling the hemodynamic response function in fMRI: efficiency, bias and mis-modeling." *Neuroimage* 45.1 (2009): S187-S198.
- [8] Rosa, Paulo N., Patricia Figueiredo, and Carlos J. Silvestre. "On the distinguishability of HRF models in fMRI." *Frontiers in computational neuroscience* 9 (2015): 54.